

Supporting Information

Realisation and optical engineering of linear variable bandpass filters in nanoporous anodic alumina photonic crystals

Sukarno^a, Cheryl Suwen Law^{a,b,c} and Abel Santos^{a,b,c*}

^aSchool of Chemical Engineering, The University of Adelaide, Engineering North Building, 5005 Adelaide, Australia

^bInstitute for Photonics and Advanced Sensing (IPAS), The University of Adelaide, 5005 Adelaide, Australia.

^cARC Centre of Excellence for Nanoscale BioPhotonics (CNBP), The University of Adelaide, 5005 Adelaide, Australia.

*E-Mail: abel.santos@adelaide.edu.au

**Realisation and optical engineering of linear variable bandpass filters
in nanoporous anodic alumina photonic crystals**

$t_{Etching}$ (min)	<i>Withdraw Speed</i> ($\mu\text{m s}^{-1}$)
2	8.3
3	5.6
4	4.2
5	3.3
6	2.8
7	2.4
8	2.0
9	1.9
10	1.7

Table S1. Correlation between etching time ($t_{Etching}$) and dip coating withdraw rate used to produce the NAA-LVBPFs analysed in our study (NB: the diameter of NAA-LVBPFs was 10 mm).

**Realisation and optical engineering of linear variable bandpass filters
in nanoporous anodic alumina photonic crystals**

2 min	3 min	4 min	5 min	6 min	7 min	8 min	9 min	10 min
(1,200,34)	(20,207,58)	(20,200,58)	(21,202,61)	(1,206,16)	(1,67,107)	(46,103,162)	(10,101,216)	(18,81,253)
(1,219,41)	(20,204,61)	(20,200,60)	(20,210,72)	(1,248,47)	(3,77,157)	(51,107,187)	(14,98,253)	(35,79,253)
(1,222,47)	(20,208,64)	(20,207,69)	(20,222,105)	(1,225,104)	(3,88,217)	(60,101,217)	(31,85,254)	(52,58,254)
(1,218,54)	(20,220,79)	(20,221,96)	(20,235,154)	(1,149,170)	(4,83,251)	(71,94,243)	(50,65,254)	(67,21,254)
(1,227,72)	(20,236,108)	(20,229,134)	(20,234,196)	(1,103,220)	(16,63,254)	(7,76,248)	(62,31,254)	(54,1,253)
(1,238,109)	(20,233,153)	(20,236,171)	(20,215,212)	(12,92,253)	(45,51,253)	(78,36,232)	(78,1,254)	(25,1,203)
(1,235,177)	(20,230,176)	(20,238,202)	(27,151,240)	(42,77,253)	(106,16,254)	(70,16,200)	(73,1,254)	(11,2,60)
(5,218,181)	(20,235,192)	(20,207,222)	(47,126,253)	(51,56,254)	(81,1,254)	(42,13,135)	(28,5,135)	(7,4,7)

(180, 94, 34)	(149,155,23)	(170, 137, 31)	(103,212,2)	(121,157,3)	(94,54,1)	(82,118,1)	(119,185,1)	(18,246,35)
(166, 102, 36)	(135,179,32)	(159,117,11)	(116,204,2)	(142,193,5)	(81,154,2)	(99,146,1)	(122,202,3)	(4,237,94)
(154, 117, 36)	(90,211,52)	(111,165,15)	(136,218,1)	(148,218,4)	(36,207,26)	(93,211,1)	(69,232,13)	(8,211,159)
(170, 137, 31)	(94,217,52)	(105,199,20)	(56,243,36)	(98,225,16)	(13,216,41)	(88,226,1)	(79,230,31)	(19,191,183)
(180,156, 27)	(94,220,52)	(106,216,21)	(57,236,42)	(56,223,30)	(8,230,50)	(89,226,2)	(36,249,109)	(21,172,183)
(176,179,25)	(88,223,55)	(101,224,25)	(78,232,45)	(33,224,45)	(7,253,69)	(43,236,49)	(32,245,166)	(19,157,172)
(156, 189,27)	(153,209,46)	(97,227,26)	(54,239,63)	(9,233,97)	(16,248,138)	(18,226,137)	(28,240,188)	(28,149,203)
(154, 191, 36)	(148,221,60)	(105,235,25)	(64,238,80)	(26,237,151)	(6,244,168)	(9,205,187)	(26,247,200)	(25,159,239)

(81, 71, 65)	(69, 55, 56)	(101, 72, 74)	(81, 65, 65)	(49, 41, 40)	(59, 46, 43)	(67, 50, 50)	(56, 37, 37)	(45, 37, 37)
(92, 78, 75)	(103, 74, 77)	(127, 80, 81)	(78, 57, 58)	(69, 36, 38)	(87, 61, 63)	(104, 42, 43)	(62, 30, 33)	(80, 29, 30)
(120, 100, 99)	(122, 74, 78)	(148, 75, 78)	(115, 60, 65)	(143, 44, 44)	(131, 57, 60)	(202, 52, 39)	(136, 31, 28)	(204, 52, 29)
(122, 100, 97)	(156, 69, 71)	(186, 73, 71)	(194, 65, 62)	(227, 69, 45)	(230, 81, 58)	(254, 108, 28)	(235, 75, 24)	(251, 101, 15)
(122, 93, 93)	(196, 67, 64)	(236, 87, 66)	(245, 85, 54)	(254, 114, 36)	(254, 122, 44)	(254, 157, 4)	(252, 123, 6)	(254, 144, 1)
(135, 95, 98)	(230, 80, 62)	(254, 102, 59)	(254, 114, 41)	(254, 147, 12)	(254, 148, 15)	(254, 206, 1)	(247, 165, 1)	(248, 208, 3)
(150, 93, 99)	(254, 109, 58)	(254, 121, 38)	(254, 138, 28)	(254, 178, 2)	(254, 179, 1)	(254, 252, 11)	(245, 225, 5)	(250, 235, 10)
(198, 98, 98)	(254, 135, 53)	(254, 151, 23)	(254, 147, 23)	(254, 207, 3)	(248, 233, 8)	(255, 255, 40)	(254, 252, 23)	(207, 222, 38)

Table S2. Correlation between interferometric colour and RGB values obtained by analysing 1 mm² areas along the etching path of NAA-LVBPFs (top – $T_p = 650$ s, centre – $T_p = 750$ s, and bottom – $T_p = 850$ s).

**Realisation and optical engineering of linear variable bandpass filters
in nanoporous anodic alumina photonic crystals**

T_P (s)	Fitting Line	R^2
650	λ_{C-PSB} (nm) = 7.4 · $t_{Etching}$ (min) + 4.8	0.9944
750	λ_{C-PSB} (nm) = 7.7 · $t_{Etching}$ (min) + 17.4	0.9963
850	λ_{C-PSB} (nm) = 15.5 · $t_{Etching}$ (min) - 12.5	0.9087

Table S3. Values of linear correlation (linear fittings shown in Figure S1) between the position of the central wavelength (λ_{C-PSB}) and the etching time ($t_{Etching}$) for NAA-LVBPFs produced with T_P = 650, 750, and 850 s.

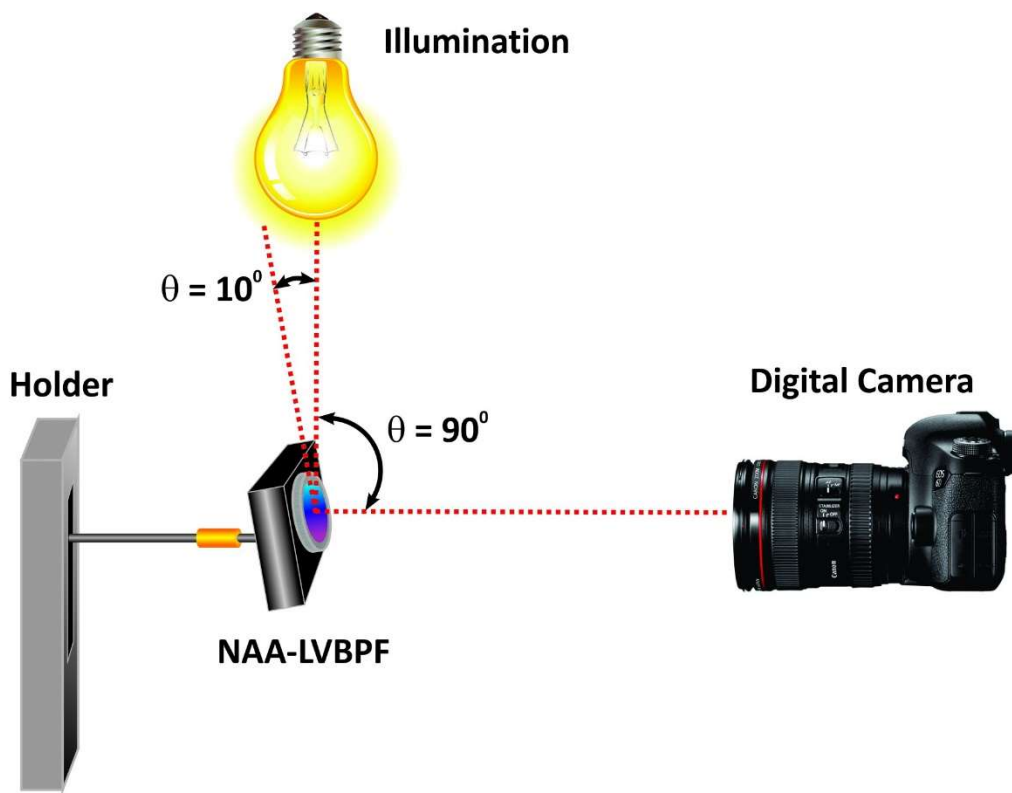


Figure S1. Schematic showing the position of the different elements (digital camera, illumination, and NAA-LVBPF) used to acquire digital images of NAA-LVBPFs.

Realisation and optical engineering of linear variable bandpass filters
in nanoporous anodic alumina photonic crystals

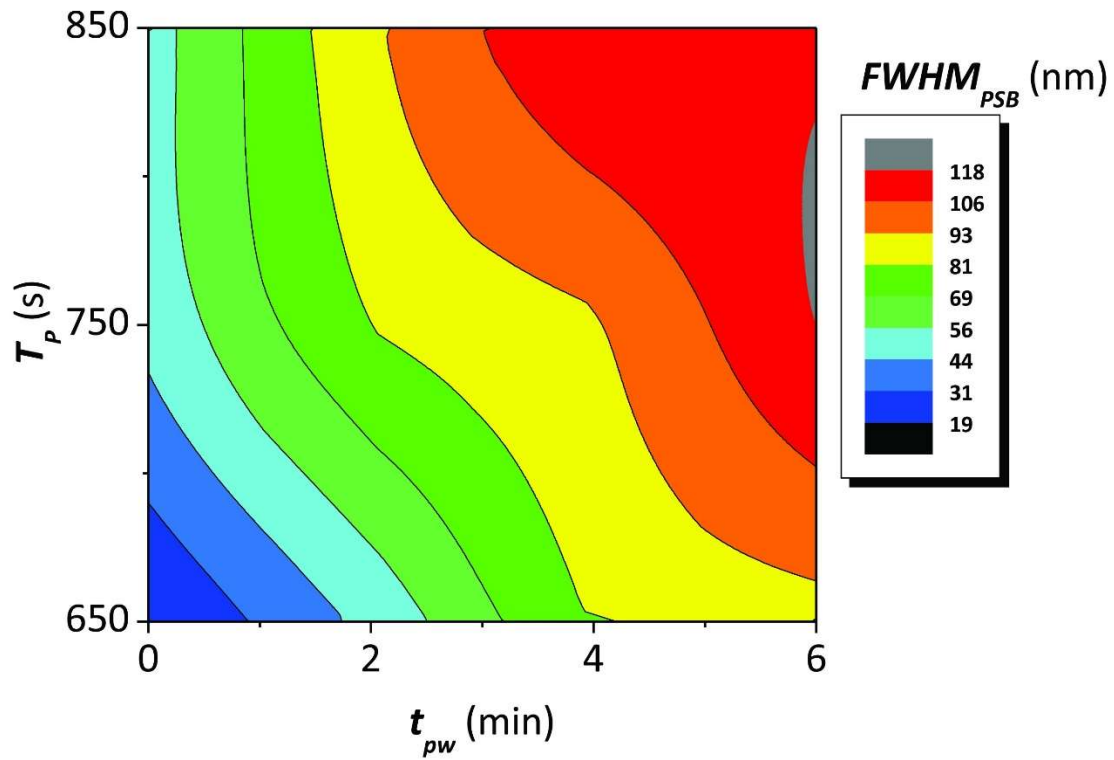


Figure S2. Dependence of the FWHM of the photonic stopband of NAA-LVBPFs produced with $T_p = 650, 750,$ and 850 s with the etching time, for $t_{Etching} = 0, 2, 4,$ and 6 min.

Realisation and optical engineering of linear variable bandpass filters
in nanoporous anodic alumina photonic crystals

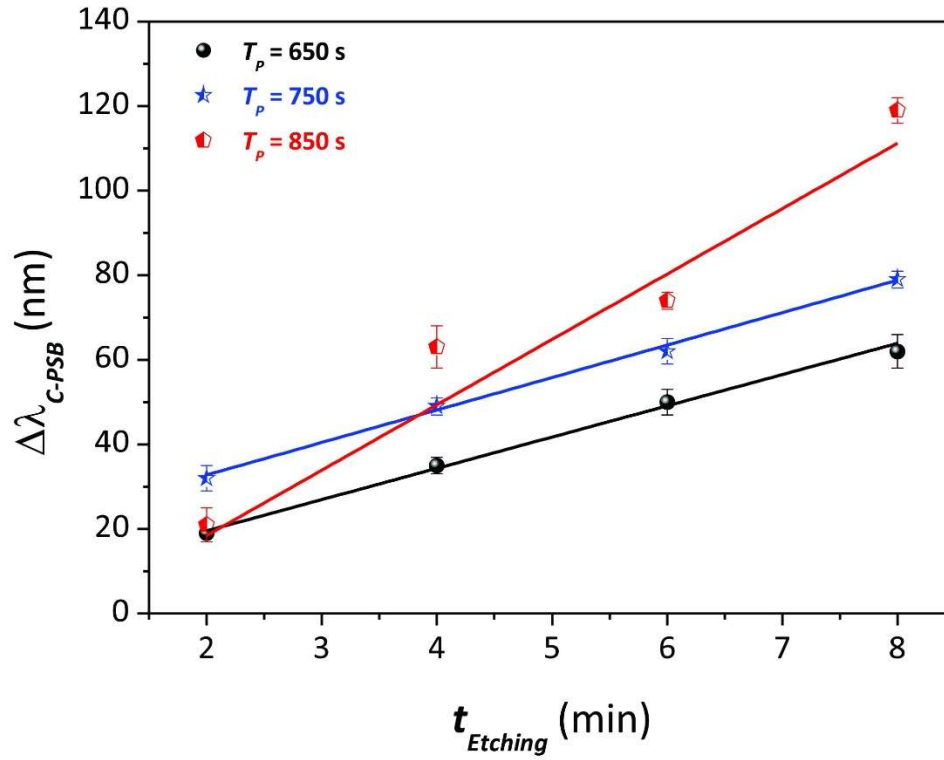


Figure S3. Linear correlation between the position of the central wavelength (λ_{C-PSB}) and the etching time ($t_{Etching}$) for NAA-LVBPFs produced with $T_p = 650, 750,$ and 850 s.